Diagram expansions in classical stochastic field theory. II. Diagram series and stochastic differential equations.

L. I. Plimak, M. Fleischhauer[†] and M. J. Collett

Dept. of Physics, University of Auckland, Private Bag 92019, Auckland, New Zealand
[†]Sektion Physik, Ludwig-Maximilians Universität München, D-80333 München, Germany

Abstract. We show that the solution to an arbitrary c-number stochastic differential equation (SDE) can be represented as a diagram series. Both the diagram rules and the properties of the graphical elements reflect causality properties of the SDE and this series is therefore called a causal diagram series. We also discuss the converse problem, i.e. how to construct an SDE of which a formal solution is a given causal diagram series. This then allows for a nonperturbative summation of the diagram series by solving this SDE, numerically or analytically.

PACS numbers: 03.70+k,05.30.Jp,05.10.Gg,11.10.Gh

Short title: Diagrams and SDEs

November 13, 1999

1. Introduction.

In our previous paper [1] (hereinafter referred to as paper I), relations called *causal Wick's theorems* were derived which express formal solutions to problems in classical stochastic field theory (CFT) as differential operations. In this paper we further re-express these solutions in the form of so-called *causal diagram series*. We discuss some structural properties of these series, including how they depend on the nature of the stochastic problem in question, or, more specifically, on the form of the stochastic differential equation (SDE) describing this problem (on SDEs see [2]). This discussion allows us then to approach the true goal of this paper: to learn how to sum a diagram series by deriving a stochastic differential equation, such that its formal solution is represented by this series. Solving this equation, numerically or analytically, is then by construction equivalent to an (in principle exact) summation of the diagram series.

As is known from quantum field theory, a diagram series may be regarded as a perturbative expansion of a path integral [3, 4]. Constructing an SDE related to this series means that this integral is re-expressed as an average over random trajectories (paths) generated by the SDE. This provides a method of calculating nontrivial path integrals numerically [5, 6], or, if the SDE happens to be soluble, even analytically [7]. In more detail this relation between diagram series, SDEs and path integrals was discussed in the introduction to paper I.

This paper is structured as follows. In Section 2, we summarise some results of paper I and show that a formal solution to an SDE may be expressed as a *causal diagram series*. In Section 3 diagram structures corresponding to certain types of problems of CFT are presented (linear or nonlinear, regular or stochastic). Finally, in Section 4 we discuss how to construct a SDE for a given causal diagram series.

2. Causal diagram series

2.1. Classical stochastic scattering problem

In paper I, we considered an (in general, stochastic) differential equation for a c-number field $\psi(r,t)$,

$$\mathcal{L}\psi(r,t) = s(r,t), \tag{1}$$

where $\mathcal{L}$ is a certain differential operator and the (in general, random) source s may depend on the field ψ. Formally solving (1) yields an integral equation,

$$\psi(r,t) = \int_{-\infty}^{\infty} dt' \int dr' G(r,r',t-t')s(r',t') + \psi_0(r,t), \tag{2}$$

where $G(r,r',t-t')$ is the retarded Green's function of equation (1),

$$\mathcal{L}G(r,r',t-t') = \delta(r-r')\delta(t-t'), \quad G(r,r',t-t') = 0, t < t', \tag{3}$$

ψ_0 being the *in*-field, $\mathcal{L}\psi_0(r,t) = 0$, and $\psi = \psi_0$ before the source is on. For simplicity, in this paper we confine ourselves to the case of a real field.

If the noise source $s(r,t)$ is singular (e.g. contains white noise [2]), equations (1) and (2) may be only symbolic. As a means of specifying stochastic calculus, one may design a *regularisation procedure* when G or s (or both) are replaced by regularised, that is, properly smoothed, functions; regularisations leading to Ito or Stratonovich calculus were discussed in paper I. For purposes of this paper, the exact regularisation procedure is mostly irrelevant. Unless stated otherwise, we assume that equations (1) and (2) are regularised in such a way that the source s and the Green's function G become infinitely differentiable, while the causality condition (3) is maintained. This also means that the integral equation (2) rather than the differential equation (1) is considered. It should be stressed, however, that while the details of regularisation are irrelevant, its presence is crucial: the causal Wick's theorem found in paper I holds only for regularised equations. This means that, unlike in QFT, the introduction of diagrams in CFT already requires regularisation.

Using the causal Wick's theorem, a formal solution to the *regularised* equation (2) was obtained in paper I, which reads

$$\Phi(\zeta) = \exp\left(\frac{\delta}{\delta\psi}G\frac{\delta}{\delta\alpha}\right)\exp\left(\zeta\psi\right)S(\alpha|\psi)\Big|_{\alpha=0,\psi=\psi_0}. \tag{4}$$

We use a condensed notation in which, e.g., $\zeta\psi = \int dx\zeta(x)\psi(x)$, where $x = \{r,t\}$ and $\int dx = \int drdt$, etc. The functional $S(\alpha|\psi)$ characterises the source in its dependence on the local (microscopic) field $\psi(r,t)$: $S(\alpha|\psi) = \overline{\mathrm{e}^{\alpha s}}\big|_\psi$ where $\overline{\cdots}\big|_\psi$ denotes statistical averaging conditional on the local field ψ. That is, regarded as a functional of $\alpha(r,t)$, $S(\alpha|\psi)$ is the characteristic functional of source averages conditioned on the local field. It depends on ψ as a parameter. Similarly, $\Phi(\zeta) = \Phi(\zeta|\psi_0) = \overline{\mathrm{e}^{\zeta\psi}}\Big|_{\psi_0}$ is the characteristic functional of the field averages, conditioned on the *in*-field. The dependence of ψ on ψ_0 corresponds to a macroscopic field-scattering problem.

The functional $S(\alpha|\psi)$ may be conveniently written in terms of *susceptibilities* $\chi^{(m,n)}(x_1,\cdots,x_m;x'_1,\cdots,x'_n)$, which are coefficients in the series expressing *cumulants* of the local source $s(x)$ in terms of the powers of the local field $\psi(x)$:

$$S(\alpha|\psi) = \exp\sum_{m,n=0}^{\infty}\frac{1}{m!n!}\alpha^m\chi^{(m,n)}\psi^n, \tag{5}$$

where $\alpha\chi^{(1,1)}\psi = \int dxdx'\,\alpha(x)\chi^{(1,1)}(x,x')\psi(x')$ etc. The susceptibilities obey the causality condition,

$$\chi^{(m,n)}(x_1,\cdots,x_m;x'_1,\cdots,x'_n) = 0, \quad \max(t'_1,\cdots,t'_n) > \max(t_1,\cdots,t_m), \tag{6}$$

i.e., the latest argument of a susceptibility is always an output one.

2.2. Diagrams for field averages.

We now show that the formal solution (4) to equations (1) or (2) may be expressed as diagram series. To be specific, we consider the case of only $\chi^{(1,0)}$, $\chi^{(1,1)}$, $\chi^{(1,2)}$, $\chi^{(2,0)}$, $\chi^{(2,1)}$ and $\chi^{(2,2)}$ non-zero; these are exactly the susceptibilities shown explicitly in equations (13), (14) in paper I. In section 4 we show that there indeed exists a stochastic problem described by this set of susceptibilities. The converse is not true: an arbitrary set of susceptibilities does not correspond to a stochastic problem. However, for purposes of this section this is irrelevant. The exact question we are concerned with is the relation between the generating expression (4) and the corresponding series, that is, how analytical elements in (4) become graphical elements. Somewhat more physical a discussion of how stochastic problems are related to diagram series may be found in sections 3 and 4.

Graphically, the Green's function $G(x;x')$ (cf equation (2)) and the *in*-field $\psi_0(x)$ will be denoted as lines,

$G(x;x') = \Big\{$ 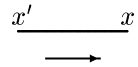

$\Big\},$ (7)

$\psi_0(x) = \Big\{$ 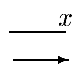

$\Big\},$ (8)

and the argument of the characteristic functional (4), $\zeta(x)$, and the susceptibilities $\chi^{(m,n)}$ will be denoted as vertices,

$\zeta(x) = \Big\{$ 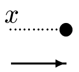

$\Big\},$ (9)

$\chi^{(1,0)}(x) = \Big\{$ 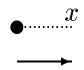

$\Big\},$ (10)

$\chi^{(1,1)}(x;x') = \Big\{$ 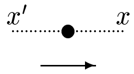

$\Big\},$ (11)

$\chi^{(1,2)}(x;x',x'') = \Big\{$ 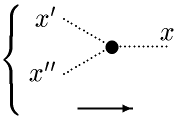

$\Big\},$ (12)

$\chi^{(2,0)}(x,x') = \Big\{$ 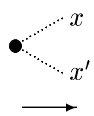

$\Big\},$ (13)

$\chi^{(2,1)}(x,x';x'') = \Big\{$ 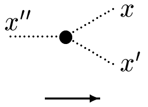

$\Big\},$ (14)

$\chi^{(2,2)}(x_1,x_2;x_1',x_2') = \Big\{$ 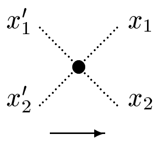

$\Big\}.$ (15)

The curly brackets isolate diagrams visually when these are used as parts of the formulae. The "time arrow" drawn below each diagram distinguishes graphically input and output arguments of the lines and vertices: The argument of $\psi_0(x)$ is regarded as a *line output*, as is the "future" argument (i.e., x) in $G(x;x')$; the "past" argument (i.e., x') in $G(x;x')$ is regarded as a *line input*. A generalised susceptibility, $\chi^{(m,n)}(x_1,\cdots,x_m;x'_1,\cdots,x'_n)$, is a quantity with n *vertex inputs* and m *vertex outputs* (marked by the dotted lines). By definition, the argument of $\zeta(x)$ is a vertex input.

We now expand all exponents in the generating expression (4) in power series, and consider a particular term in these series. It is easy to see that $\alpha(x)$ always occurs convolved with a vertex output, while $\frac{\delta}{\delta\alpha(x)}$ is always convolved with a line input. Since $\frac{\delta\alpha(x)}{\delta\alpha(x')} = \delta(x-x')$, differentiating by α's leaves all vertex outputs pairwise convolved with line inputs. No free vertex outputs or line inputs may remain; terms with unequal number of these give zero. Similarly, derivatives $\frac{\delta}{\delta\psi(x)}$ leave vertex inputs convolved with the line outputs of the propagators $G(x;x')$; surviving ψ's become ψ_0's. As a result, we find all vertex inputs pairwise convolved with line outputs, and *vice versa*, and no free arguments remain. Graphically, convolved input-output pairs will be denoted by connecting respective ends of the lines to the vertices, e.g.,

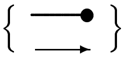

$$= \int dx\, \zeta(x)\psi_0(x), \tag{16}$$

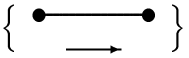

$$= \int dx dx'\, \zeta(x)G(x;x')\chi^{(1,0)}(x'), \tag{17}$$

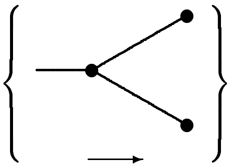

$$= \int dx_1 \cdots dx_5\, \zeta(x_1)\zeta(x_2)G(x_1;x_3)G(x_2;x_4)\chi^{(2,1)}(x_3,x_4;x_5)\psi_0(x_5), \tag{18}$$

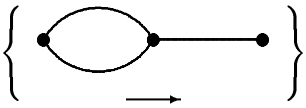

$$= \int dx_1 \cdots dx_6\, \zeta(x_1)G(x_1;x_2)\chi^{(1,2)}(x_2;x_3,x_4)G(x_3;x_5)G(x_4;x_6)\chi^{(2,0)}(x_5,x_6). \tag{19}$$

Expressions of such structure will be called *causal diagrams*. Note that the time arrow applies to all elements in a diagram.

In general, a causal diagram is a product of the basic elements—lines and vertices, where *some* line inputs and outputs are pairwise convolved with, respectively, vertex outputs and inputs. A diagram containing free arguments will be called *incomplete*; (7–15) are legitimate incomplete diagrams. A diagram without free arguments is *complete*; examples of complete diagrams are (16–19).

Expanding (4) thus yields an expression for the functional $\Phi(\zeta)$ as a sum of all complete causal diagrams which may be built out of the elements (7–15). The coefficients with which diagrams occur in the series are equal to one over the order of the symmetry group of the graph (symmetry coefficients) [3]. Incomplete diagrams occur e.g in diagram expansions for the field averages. Formally, they are found by stripping the ζ vertices from the complete diagrams. The simplest example of such a diagram is (8): it contributes to $\overline{\psi(r,t)}$ and is found by stripping the ζ vertex from (16).

Note that by virtue of our assumption that the free Green's function as well as the source are infinitely differentiable, the diagrams introduced cannot contain ultraviolet divergences. However, weaker assumptions may suffice, e.g. that all susceptibilities are local and contain only the delta-function and its derivatives up to a given order, while G is infinitely differentiable. It is also clear that to make a particular diagram convergent G has only to have a finite number of continuous derivatives. Whether this would suffice to make any diagram convergent will be discussed in connection with particular problems.

It is worth noting that whereas in diagrams the "time flow" is from left to right, in analytical expresssions, as a rule, time increases from right to left. For example, in the diagram in (17) the ζ vertex is on the right, whereas in the analytical expression $\zeta G\chi^{(1,0)} = \int dxdx'\zeta(x)G(x;x')\chi^{(1,0)}(x')$ the natural position of the function $\zeta(x)$ is on the left. Thus objects are commonly in reverse order in diagrams and analytical notation.

2.3. Connected diagrams and field cumulants.

A diagram that graphically consists of a number of separate subdiagrams without common elements is called *disconnected*; otherwise, it is *connected*. A disconnected diagram is a product of its connected components. In the above examples, all diagrams are connected; however, the causal diagram series for the functional $\Phi(\zeta)$ contains *all* possible complete diagrams, connected as well as disconnected.

To get rid of disconnected diagrams, one should describe the field in terms of its *cumulants* rather than averages. Formally, the field cumulants $C^{(n)}, n = 0, 1, \cdots$, are defined as,

$$\Phi(\zeta) = \exp \sum_{n=1}^{\infty} \frac{1}{n!}\zeta^n C^{(n)}, \tag{20}$$

where $\zeta C^{(1)} = \int dx\, \zeta(x) C^{(1)}(x)$ etc. In particular,

$$\overline{\psi(x)} = C^{(1)}(x), \tag{21}$$

$$\overline{\psi(x)\psi(x')} = C^{(2)}(x,x') + C^{(1)}(x)C^{(1)}(x'), \tag{22}$$

$$\begin{aligned}\overline{\psi(x)\psi(x')\psi(x'')} = {} & C^{(3)}(x,x',x'') + C^{(2)}(x,x')C^{(1)}(x'') + C^{(2)}(x,x'')C^{(1)}(x') \\ & + C^{(2)}(x',x'')C^{(1)}(x) + C^{(1)}(x)C^{(1)}(x')C^{(1)}(x''),\end{aligned} \tag{23}$$

$$\vdots$$

i.e., expression of a particular field average by the cumulants corresponds to summing all its possible factorisations. Characterisation of the field statistics by cumulants is more economical than characterisation by field averages. E.g., if $\psi(x)$ is non-random, $C^{(1)}(x) = \psi(x)$, and $C^{(n)} = 0, n > 1$; if $\psi(x)$ is random and Gaussian, its cumulants vanish for $n > 2$; whereas all field averages are non-zero even for non-random ψ.

There exists a general theorem (Mayer's first theorem) [3] stating that the diagram expansion of the logarithm of $\Phi(\zeta)$ contains only connected diagrams, so that

$$\Phi(\zeta) = \exp[\mathrm{conn}\Phi(\zeta)], \tag{24}$$

where $\mathrm{conn}\Phi(\zeta)$ is given by diagram series where all disconnected diagrams are dropped while connected ones retain their coefficients. Comparing this with the definition of the field cumulants, we see that

$$\mathrm{conn}\Phi(\zeta) = \ln\Phi(\zeta) = \sum_{n=1}^{\infty} \frac{1}{n!}\zeta^n C^{(n)}. \tag{25}$$

Hence a diagram expansion for $\frac{1}{n!}\zeta^n C^{(n)}$ contains all connected complete diagrams with exactly n ζ-vertices (9), occurring with the coefficients they had in the series for $\Phi(\zeta)$. The expansion for $C^{(n)}(x_1, \cdots, x_n)$ contains all connected incomplete causal diagrams, which do not contain ζ vertices and have exactly n free line outputs.

3. Diagram structures corresponding to certain types of equations.

3.1. Emission of given sources.

To start with, we consider the simplest possible stochastic problem of radiation of a *given random* source, $s(x) = s_0(x)$. For simplicity, we assume that it is Gaussian, and described by the cumulants $\overline{s_0(x)} = \chi^{(1,0)}(x)$ and $\overline{s_0(x)s_0(x')} - \overline{s_0(x)}\;\overline{s_0(x')} = \chi^{(2,0)}(x,x')$ (conditioning on the full field is irrelevant for a given source). This problem is readily solved:

$$\psi(x) = \psi_0(x) + \int dx' G(x;x') s_0(x'). \tag{26}$$

For the field cumulants we have,

$$C^{(1)}(x) = \psi_0(x) + \int dx' G(x;x')\chi^{(1,0)}(x') = \left\{ \quad \right\} + \left\{ \quad \right\}, \tag{27}$$

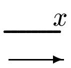

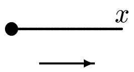

$$C^{(2)}(x,x') = \int dx'' dx''' G(x;x'')G(x';x''')\chi^{(2,0)}(x'',x''') = \left\{ \quad \right\}, \tag{28}$$

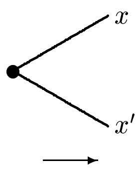

so that,

$$\ln \Phi(\zeta) = \zeta C^{(1)} + \frac{1}{2}\zeta^2 C^{(2)} =$$ 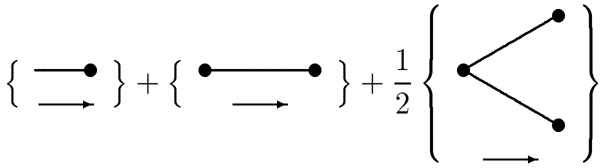 . (29)

It is easy to see that these are indeed the three (and only three) connected complete diagrams that can be built of the available graphical elements ψ_0, G, $\chi^{(1,0)}$ and $\chi^{(2,0)}$, and that the symmetry coefficients are also correct. Hence expressions (27–29) are exactly that one would find from the diagrammatic approach. Note, however, that the logic of the diagrammatic solution is reversed: relation (29) is found summing all legitimate complete connected diagrams, and relations (27–28) follow from it.

3.2. Linear susceptibility.

Consider now an equation with a nonzero linear susceptibility, $\chi^{(1,1)}(x; x') \neq 0$. For simplicity, we assume that the only other non-zero susceptibility is $\chi^{(1,0)}(x)$, i.e., we consider radiation from a given nonrandom source into a linear medium. The following considerations are nevertheless applicable in a general case of any set of nonzero susceptibilities.

All connected diagrams containing only the vertices $\chi^{(1,1)}(x; x')$ and $\chi^{(1,0)}(x)$ are *chains*,

$$\ln \Phi(\zeta) =$$ 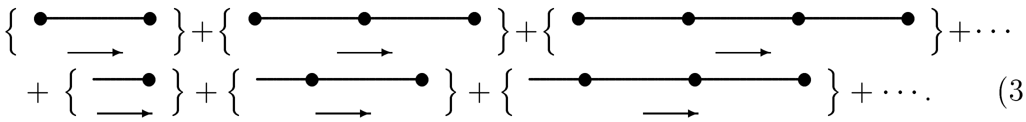 (30)

On their "past" end, the chains are terminated either by the vertex $s_0 = \chi^{(1,0)}$,

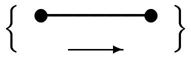 $= \zeta G \chi^{(1,0)}$, (31)

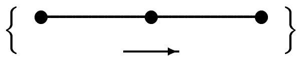 $= \zeta G \chi^{(1,1)} G \chi^{(1,0)}$, (32)

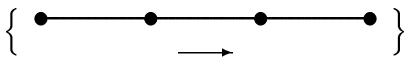 $= \zeta G \chi^{(1,1)} G \chi^{(1,1)} G \chi^{(1,0)}$, (33)

$\vdots$

or by the line ψ_0,

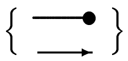 $= \zeta \psi_0$, (34)

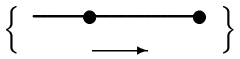 $= \zeta G \chi^{(1,1)} \psi_0$, (35)

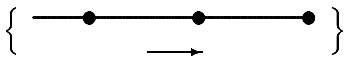 $= \zeta G \chi^{(1,1)} G \chi^{(1,1)} \psi_0$, (36)

$\vdots$

The symmetry coefficients of the chains are all equal to one. Note that there exists another class of connected diagrams, namely loops:

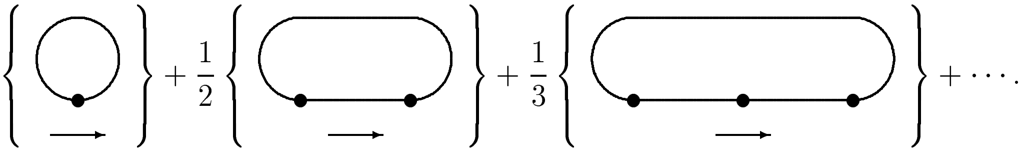

They are however zero due to causality conditions and the regularisation of G or $\chi^{(1,1)}$.

There are two possible ways that $\chi^{(1,1)}$ can appear in a diagram: (i) between two Gs, and (ii) between a ψ_0 and G; it is the former that is responsible for the infinite number of chains. Consider the sum of chains

$G'(x;x') =$

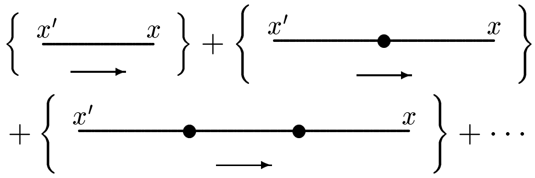

$$= G(x;x') + \int dx''dx'''G(x;x'')\chi^{(1,1)}(x'';x''')G(x''';x') + \cdots. \tag{37}$$

It obeys an integral (Dyson) equation,

$$G' = G + G\chi^{(1,1)}G'. \tag{38}$$

Acting on it with the operator $\mathcal{L}$, and using the fact that $\mathcal{L}G = \mathcal{I}$ ($\mathcal{I}$ here is an identity operator), we find

$$\mathcal{L}'G' \equiv (\mathcal{L} - \chi^{(1,1)})G' = \mathcal{I}. \tag{39}$$

Thus partial summation of the chains in diagrams corresponds to shifting the linear susceptibility from the source to the free equation. Replacing $G \to G'$ allows one to drop all diagrams containing a $\chi^{(1,1)}$ vertex between two G lines. The $\chi^{(1,1)}$ vertices placed between ψ_0s and Gs are only found in the combination

$\psi_0'(x) =$ 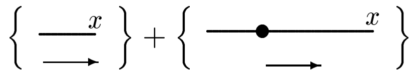 (40)

where the propagator is now G'. We see that $\mathcal{L}\psi_0 = 0$ is equivalent to $\mathcal{L}'\psi_0' = 0$. Hence by redefining the graphical notation,

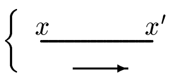 $= G'(x;x')$, 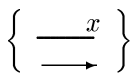 $= \psi_0'(x)$, 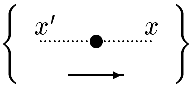 $= 0$, (41)

(and dropping the primes) we arrive at an equivalent problem where the linear susceptibility is included into the operator $\mathcal{L}$. From now on we always assume this to be the case.

Note that instead of redefining the *in*-field, one could equally redefine the $\chi^{(1,0)}$ vertex,

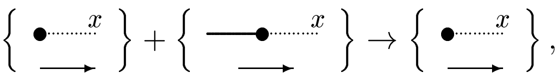 (42)

leaving ψ_0 unchanged. Then ψ_0 is no longer a solution to the free equation, but, firstly, when deriving diagrams using Eq. (4) this fact is irrelevant, and secondly, $\mathcal{L}\psi_0 = 0$ (and hence $\mathcal{L}'\psi_0' = 0$) will typically not hold with regularisation.

3.3. Nonlinear deterministic equations.

We now consider an equation with quadratic nonlinearity, $\chi^{(1,2)} \neq 0$. We assume that this equation is non-stochastic, $\chi^{(2,0)} = \chi^{(2,1)} = 0$, and that $\chi^{(1,1)} = 0$ (or is included in the operator $\mathcal{L}$). The available graphical elements hence are then $\psi_0, G, \chi^{(1,0)}$ and $\chi^{(1,2)}$; with two exceptions, all connected diagrams that one can build using these elements are trees branching into the past:

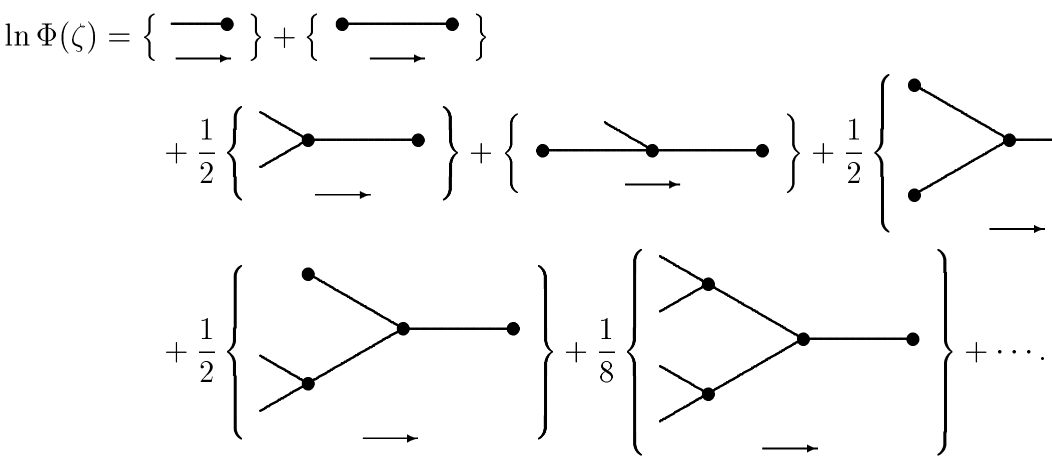

(43)

The futuremost vertex in the trees is ζ, branching occurs at $\chi^{(1,2)}$ vertices, and branches are ultimately terminated by ψ_0 lines or $\chi^{(1,0)}$ vertices. The series (43) contains all such trees, each with a symmetry coefficient one over the order of the symmetry group of the tree.

3.4. Stochastic differential equations.

Consider firstly a special case when $\chi^{(m,n)} = 0$ for $n > 1$ (note that this does not correspond to any stochastic problem in the true meaning of the word). Connected diagrams are then trees branching into the future:

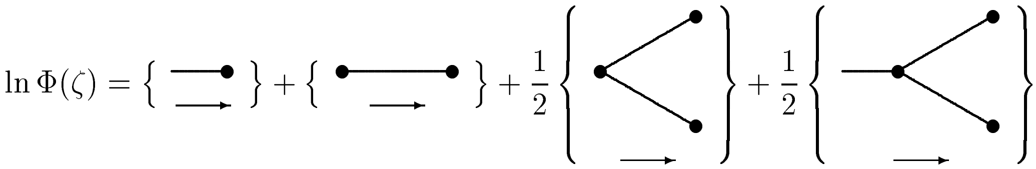

(44)

$+\frac{1}{2}$ 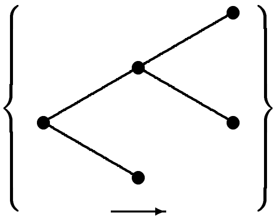 $+\frac{1}{2}$ 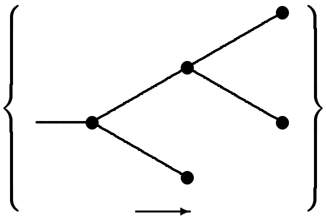 $+\frac{1}{8}$ 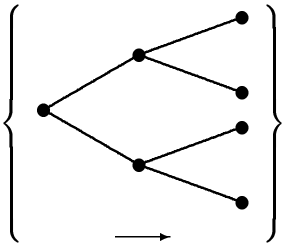 $+\cdots.$

It is clear that diagrams with arbitrary number of ζ vertices may be found in this series. Hence, despite the fact that the local source conditioned on the full radiated field is Gaussian, the radiated field itself is non-Gaussian: it has non-zero cumulants $C^{(n)}$ for all n. The number of connected diagrams is infinite, yet the diagram series retains a certain tameness; e.g., the number of diagrams contributing to each field cumulant, $C^{(n)}$, is still finite.

The final (and crucial) step leading to truly nontrivial series is combining nonlinearity and noise. Assume first that $\chi^{(2,2)} = 0$. Among the connected diagrams produced by relation (4), we find all trees, both nonlinear (43) and stochastic (44); on top of that, we find a totally new class of netlike *diagrams with loops*:

$\ln \Phi(\zeta) = \text{Trees} + \frac{1}{2}$ 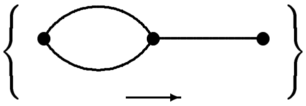 $+\frac{1}{2}$ 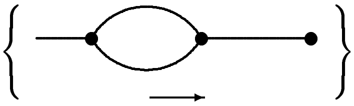

$+\frac{1}{4}$ 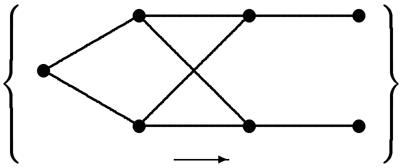 $+\frac{1}{2}$ 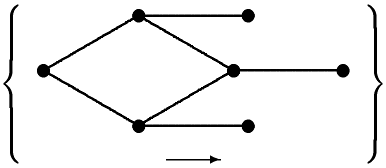

$+$ 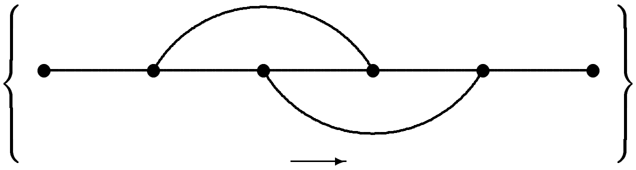 $+\cdots.$ (45)

The number of connected diagrams contributing to any field cumulant is now infinite.

Assume now that $\chi^{(2,2)} \neq 0$. Since this vertex may be attributed to both nonlinearity and noise (indeed, it contains two inputs and two outputs), diagrams with loops may originate in combining this vertex with itself. This yields diagrams like

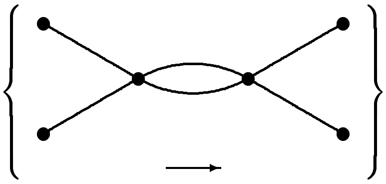 (46)

Note that whereas (44) and (45) alone do not correspond to any stochastic problem, with the inclusion of nonzero $\chi^{(2,2)}$ there are some choices of the susceptibilities which do represent stochastic processes in the true meaning of the word. We return to this question in Section 4.

3.5. Regularisation of the equation and convergence of the diagrams

If produced by a regularised equation (2), the diagrams with loops do not contain ultraviolet divergences. (Infrared divergences may still be present; however the physical reason for these is well understood and we ignore them.) In a single-mode case, regularisations are necessary to resolve uncertainties connected with the system's self-action at zero time delays (cf the discussion in paper I at the end of Section 2). For example, the following diagrams describe how the noise emitted by the medium affects its own emission producing a coherent signal and how the noise is processed by the nonlinearity before taking part in its own creation, respectively.

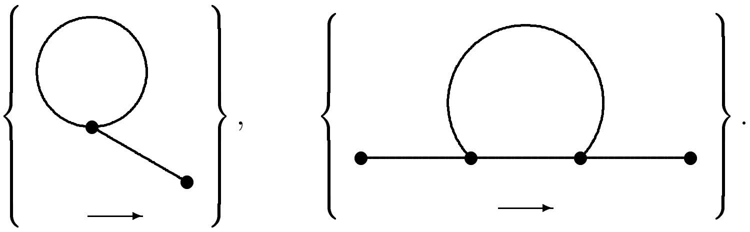

(47)

(When drawing diagrams like (47) an additional specification of the graphical notation is necessary. Namely, the input and output ends of the propagators are those pointing, respectively, towards past and future. Or, which is the same, connected, respectively, to the outputs and inputs of the vertices. Whether the output of a propagator is graphically earlier or later than the input is irrelevant.)

If the system is non-Markovian, both diagrams in (47) may describe legitimate physical processes due to multi-time correlations; these diagrams may then be convergent. We shall consider the non-Markovian case elsewhere. If the system is Markovian, i.e.,

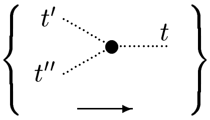

$\sim$

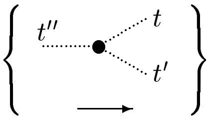

$$\sim \delta(t-t')\delta(t-t''), \tag{48}$$

both diagrams contain $G(0)$ which is undefined if (1) is first order in time. In the frequency domain, this produces a genuine ultraviolet divergence. However if $G(t)$ is replaced by $G_{\mathrm{reg}}(t)$, as is in fact necessary in order to derive the causal Wick's theorem (cf paper I), there is no uncertainty any more: $G_{\mathrm{reg}}(0) = 0$ and the above diagrams are zero. This is the case for any diagram where noise affects its own creation. Such diagrams contain a closed causal loop of propagators starting and finishing at the same vertex. They are all proportional to $[G(0)]^k$, where k is an integer, and disappear when $G(t)$ is replaced by $G_{\mathrm{reg}}(t)$. (Again, this only applies in the Markovian case; these diagrams do not necessarily disappear in non-Markovian systems.)

An important point is that regularisations are introduced in order to make mathematical sense of the equation considered, not in order to make diagrams convergent. The latter is a "side effect" of the regularisation. Strictly speaking, our approach is unable to produce divergent diagrams, because the derivation of the diagrammatic solution to equation (2) is based on the causal Wick's theorem of which the proof is in turn based on regularisations (cf paper I). Only if we ignore this, i.e., make an intentional error, do we encounter divergences in the diagrams.

In a continuous-space case, additional singularities appear in the propagator rendering more diagrams divergent. In principle, it is obvious that regularising the propagator allows one to counteract these divergences since the more continuous derivatives the regularised propagator has the faster its Fourier transform vanishes. (This is exactly how the Pauli-Villars regularisation works in QFT [8].) The remaining question is whether a given finite number of continuous derivatives would suffice to remove divergences from an arbitrary diagram. This question will be considered in another paper.

4. Converse problem: Constructing an SDE for a given causal diagram series

Assume a diagram series is given (derived in a quantum problem, say). This series appears as a causal one, i.e., is generated by an expression like (4), and the causality conditions hold for all graphical elements. Formally, the generalised susceptibilities $\chi^{(m,n)}$ then provide one with a complete and unambiguous description of the equivalent classical stochastic process. In practice, however, it would be more convenient to deal with an explicit SDE, written in terms of noise sources which are independent of the field. This leads us into the converse problem of the causal diagram techniques: how to write explicitly an SDE corresponding to a given causal diagram series.

With no stochasticity present, the relation between a causal diagram series and the corresponding DE is straightforward: a diagram series with only single-output vertices, $\chi^{(1,n)}$, solves the equation

$$\mathcal{L}\psi(x) = \sum_{n=1}^{\infty} \frac{1}{n!} \int dx_1 \cdots dx_n \chi^{(1,n)}(x; x_1, \cdots, x_n)\psi(x_1) \cdots \psi(x_n). \tag{49}$$

Basically, any SDE should look identical to this equation, with the only difference that (some of) the susceptibilities are random. It is clear that

$$\Phi(\zeta) = \overline{\Phi_0(\zeta)}, \tag{50}$$

where $\Phi(\zeta)$ is the diagram series solving (49) regarded as an SDE, $\Phi_0(\zeta)$ is the series solving (49) as a non-stochastic equation, and the upper bar here denotes averaging over the random susceptibilities in (49). The key to the converse problem is in the relation between $\Phi_0(\zeta)$ and $\Phi(\zeta)$.

Consider, to begin with, an example of a given random source. The SDE is then

$$\mathcal{L}\psi(x) = s_0(x). \tag{51}$$

For simplicity, we assume that s_0 is Gaussian with zero average, $\overline{s_0(x)} = 0$ and $\overline{s_0(x)s_0(x')} = \chi^{(2,0)}(x,x')$. Then, (implying $s_0 = \chi^{(1,0)}$)

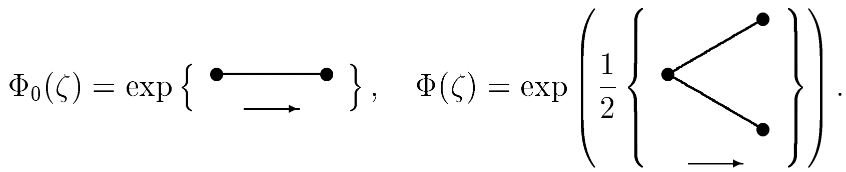

(52)

On the other hand, expanding $\Phi_0(\zeta)$ in a diagram series and performing the averaging as required by (50) in each of the diagrams separately, we find:

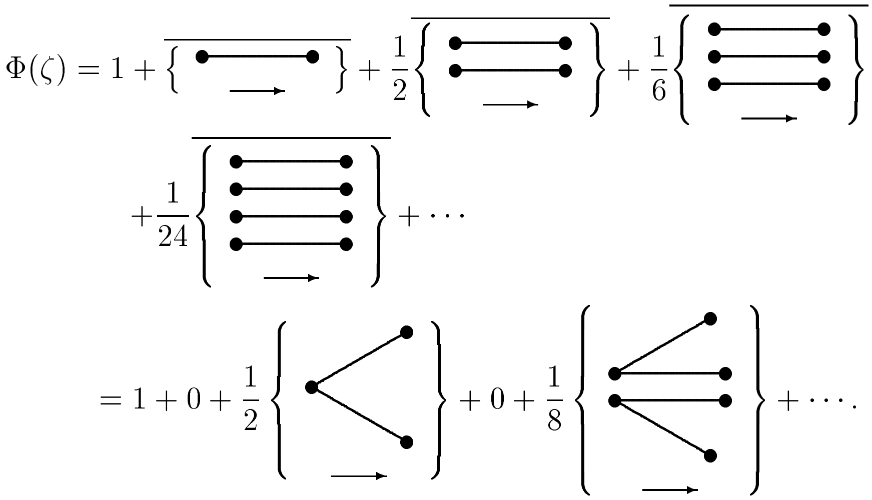

(53)

We see that the graphical operation reflecting s_0 becoming random and Gaussian is a pairwise *merging* of the $\chi^{(1,0)}$ vertices into $\chi^{(2,0)}$ vertices; diagrams with an odd number of the $\chi^{(1,0)}$ vertices become zero. Note that whereas the merging of the vertices itself reflects stochasticity, the fact that it is pairwise is clearly due to the Gaussian statistics: if s_0 were non-Gaussian, then non-zero $\chi^{(m,0)}$ vertices would each result from merging of m $\chi^{(1,0)}$ vertices.

Consider now an SDE with a multiplicative noise,

$$\mathcal{L}\psi(x) = \int dx' \chi^{(1,1)}(x;x')\psi(x') + s'(x), \tag{54}$$

where $\chi^{(1,1)}(x;x')$ is random and $s'(x)$ contains non-stochastic terms (it may also contain other noise sources provided they are not correlated with $\chi^{(1,1)}$). For simplicity, we again assume that $\chi^{(1,1)}(x;x')$ is Gaussian and $\overline{\chi^{(1,1)}(x;x')} = 0$, so that it is specified by the average $\overline{\chi^{(1,1)}(x_1;x_1')\chi^{(1,1)}(x_2;x_2')}$. The diagram series for equation (54) can be found by averaging those for an equation with a linear susceptibility $\chi^{(1,1)}(x;x')$. This is readily done directly in the generating expression (4):

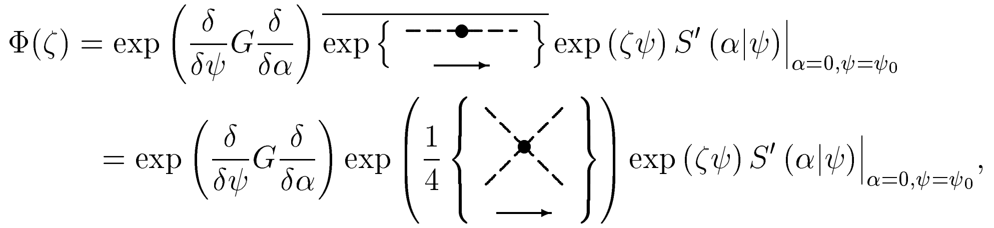

$$\Phi(\zeta) = \exp\left(\frac{\delta}{\delta\psi}G\frac{\delta}{\delta\alpha}\right)\overline{\exp\left\{ \quad \right\}}\exp\left(\zeta\psi\right)S'\left(\alpha|\psi\right)\Big|_{\alpha=0,\psi=\psi_0}$$
$$= \exp\left(\frac{\delta}{\delta\psi}G\frac{\delta}{\delta\alpha}\right)\exp\left(\frac{1}{4}\left\{ \quad \right\}\right)\exp\left(\zeta\psi\right)S'\left(\alpha|\psi\right)\Big|_{\alpha=0,\psi=\psi_0}, \tag{55}$$

where $S'(\alpha|\psi)$ contains vertices originating in $s'(x)$, and the following graphical notation is used,

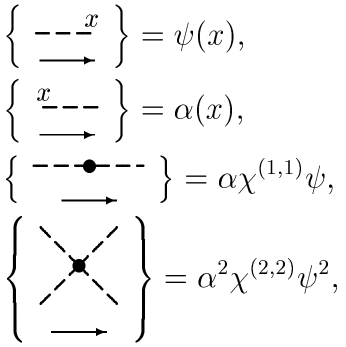

$$\left\{ \quad \right\} = \psi(x), \tag{56}$$
$$\left\{ \quad \right\} = \alpha(x), \tag{57}$$
$$\left\{ \quad \right\} = \alpha\chi^{(1,1)}\psi, \tag{58}$$
$$\left\{ \quad \right\} = \alpha^2\chi^{(2,2)}\psi^2, \tag{59}$$

where

$$\chi^{(2,2)}(x_1,x_2;x_1',x_2') = \overline{\chi^{(1,1)}(x_1;x_1')\chi^{(1,1)}(x_2;x_2')} + \overline{\chi^{(1,1)}(x_1;x_2')\chi^{(1,1)}(x_2;x_1')}. \tag{60}$$

Hence the graphical representation of the linear susceptibility becoming random is pairs of the $\chi^{(1,1)}$ vertices merging into the $\chi^{(2,2)}$ vertices, e.g.,

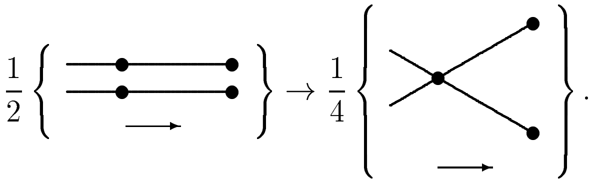

$$\frac{1}{2}\left\{ \quad \right\} \to \frac{1}{4}\left\{ \quad \right\}. \tag{61}$$

This is just the Hubbard-Stratonovich transformation used in path-integral approaches in QFT [3].

Similarly, if a certain *pair* of susceptibilities ($\chi^{(1,0)}$ and $\chi^{(1,1)}$, say) become random and correlated (assuming Gaussian), then averaging Φ_0 we get,

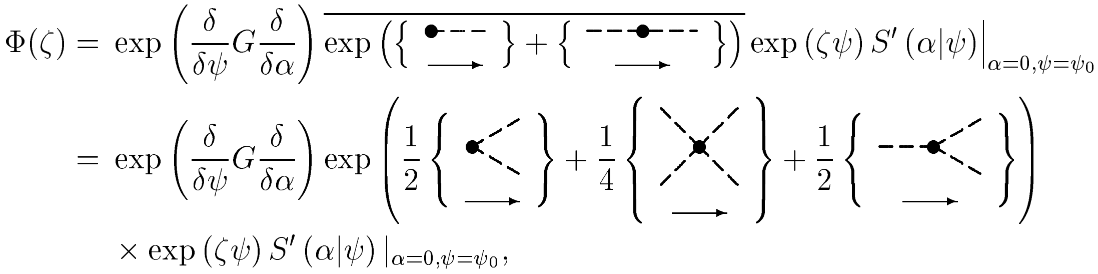

$$\Phi(\zeta) = \exp\left(\frac{\delta}{\delta\psi}G\frac{\delta}{\delta\alpha}\right)\overline{\exp\left(\left\{ \quad \right\} + \left\{ \quad \right\}\right)}\exp\left(\zeta\psi\right)S'\left(\alpha|\psi\right)\Big|_{\alpha=0,\psi=\psi_0}$$
$$= \exp\left(\frac{\delta}{\delta\psi}G\frac{\delta}{\delta\alpha}\right)\exp\left(\frac{1}{2}\left\{ \quad \right\} + \frac{1}{4}\left\{ \quad \right\} + \frac{1}{2}\left\{ \quad \right\}\right)$$
$$\times \exp\left(\zeta\psi\right)S'\left(\alpha|\psi\right)|_{\alpha=0,\psi=\psi_0}, \tag{62}$$

where

$\Big\{$ 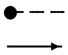 $\Big\} = \alpha\chi^{(1,0)}, \qquad (63)$

$\Big\{$ 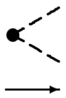 $\Big\} = \alpha^2\chi^{(2,0)}, \qquad (64)$

$\Big\{$ 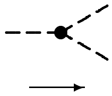 $\Big\} = \alpha^2\chi^{(2,1)}\psi, \qquad (65)$

and

$$\chi^{(2,0)}(x_1,x_2) = \overline{\chi^{(1,0)}(x_1)\chi^{(1,0)}(x_2)}, \tag{66}$$

$$\chi^{(2,1)}(x_1,x_2;x') = \overline{\chi^{(1,1)}(x_1;x')\chi^{(1,0)}(x_2)} + \overline{\chi^{(1,1)}(x_2;x')\chi^{(1,0)}(x_1)}, \tag{67}$$

see (59) and (60) as well. We see that whereas randomness results in self-mergings ($\chi^{(1,0)}+\chi^{(1,0)} \to \chi^{(2,0)}$ and $\chi^{(1,1)}+\chi^{(1,1)} \to \chi^{(2,2)}$), correlations manifest themselves as cross-mergings ($\chi^{(1,0)}+\chi^{(1,1)} \to \chi^{(2,1)}$).

Another example is

$\Phi(\zeta) = \exp\left(\frac{\delta}{\delta\psi}G\frac{\delta}{\delta\alpha}\right)\overline{\exp\Big(\Big\{}$ 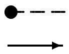 $\Big\} + \frac{1}{2}\Big\{$ 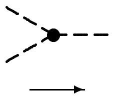 $\overline{\Big\}\Big)}\exp(\zeta\psi)\,S'(\alpha|\psi)\,|_{\alpha=0,\psi=\psi_0}$

$= \exp\left(\frac{\delta}{\delta\psi}G\frac{\delta}{\delta\alpha}\right)\exp\Big(\frac{1}{2}\Big\{$ 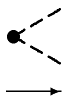 $\Big\} + \frac{1}{48}\Big\{$ 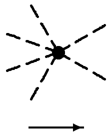 $\Big\} + \frac{1}{4}\Big\{$ 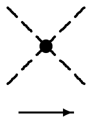 $\Big\}\Big)$

$\times \exp(\zeta\psi)\,S'(\alpha|\psi)\,|_{\alpha=0,\psi=\psi_0}, \qquad (68)$

where

$\Big\{$ 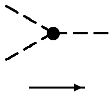 $\Big\} = \alpha\chi^{(1,2)}\psi^2, \qquad (69)$

$\Big\{$ 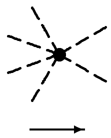 $\Big\} = \alpha^2\chi^{(2,4)}\psi^4, \qquad (70)$

and

$$\chi^{(2,4)}(x_1,x_2;x_1',x_2',x_3',x_4') = \sum_{\text{perm}}\overline{\chi^{(1,2)}(x_1;x_1',x_2')\chi^{(1,2)}(x_2;x_3',x_4')}, \tag{71}$$

where $\sum_{\text{perm}}$ denotes summation over all different terms obtained by (separate) permutations of the input and output arguments, cf (60). The rest of the notation was introduced above.

This way, if we take equation (49), derive a diagram series for it, and then assume that the susceptibilities $\chi^{(1,n)}$ are random, the new series is found from the initial series by merging certain vertices in the diagrams. Hence in order to recover the initial non-stochastic equation, the merged vertices should be factorised into the products of the initial vertices. Formally, this means solving functional equations like (60) or (66–67), with given stochastic vertices, in order to find statistics of the susceptibilities in (49). This is the well-known problem of moments in probability theory.

It is obvious that there exist causal diagram series that do not correspond to any SDE in the true meaning of the word. E.g., $\chi^{(2,0)}(x;x') = -\delta(x-x')$ would require $\overline{s_0(x)s_0(x')} = -\delta(x-x')$; this is certainly impossible in probability theory. We therefore have to adopt the concept of pseudo-probability [5] and consider pseudo-stochastic differential equations (PSDE) as well as stochastic ones. (This is anyway inevitable in quantum stochastics since the measure in Feynman path integrals is as a rule nonpositive.) Even with this generalisation, it is not clear if the converse problem has a general solution consistent with the causality conditions for the susceptibilities.

However, this clearly is the case for an important class of problems, namely, local Markovian problems. In terms of the susceptibilities, this means that they are nonzero only if all their arguments (both input and output) coincide. E.g., let $\chi^{(2,2)}(x_1,x_2;x_1',x_2') = \chi\delta(x_1-x_1')\delta(x_2-x_2')\delta(x_1-x_2)$, where χ is a real constant, positive or negative. Then, the converse problem is solved by $\chi^{(1,1)}(x;x') = \sqrt{|\chi|}\,\eta(x)\delta(x-x')$, where for $\chi > 0$ $\eta(x)$ is a standardised Gaussian δ-correlated noise source, $\overline{\eta(x)\eta(x')} = \delta(x-x')$; whereas for $\chi < 0$ $\eta(x)$ is a standardised Gaussian δ-correlated *pseudo-stochastic* source, $\overline{\eta(x)\eta(x')} = -\delta(x-x')$. Note that one can find an alternative solution using factorisation (68). This shows that a solution to a converse problem is in general *non-unique*.

Another class of series that lead to pseudo-stochastic equations are those with non-Gaussian vertices. As we have seen from the above examples, Gaussian noise sources always produce noise vertices with two outputs; such vertices are naturally termed Gaussian. Non-Gaussian vertices are those with three outputs or more; they correspond to higher-order noises [2, 5]. If a series contains a finite number of non-Gaussian vertices, it can only be interpreted in terms of a pseudo-SDE. Examples of such noises and corresponding series will be considered elsewhere.

5. Conclusion

We have shown that there exist simple rules which relate a certain class of diagram series (causal diagram series) to stochastic differential equations. This provides a tool for calculating causal diagram series non-perturbatively, e.g. by numerical simulations. Furthermore, it demonstrates that despite the apparent incompatiblity of q- and c-number techniques there exists a profound mathematical similarity between the classical stochastic and quantum field theories. For bosons this similarity can in fact be expanded to a formal identity. This will be the subject of future papers [6] (see also [7]).

Acknowledgments

M.F. would like to thank the Physics Department of The University of Auckland and Prof. D.F.Walls for hospitality during his stay at Auckland. This work was supported by the Marsden Fund of the Royal Society of New Zealand.

References

[1] Plimak L I, Fleischhauer M and Collett M J 1998, *J. Phys. A: Math. Gen.* .

[2] Gardiner C W 1985, *Handbook of stochastic methods for physics, chemistry, and the natural sciences* (Berlin-New York: Springer).

[3] Negerle J W and Orland H 1978, *Quantum Many-Particle Systems* (Reading, MA: Addision-Wesley).

[4] Wiegel F M 1975, *Path Integral Methods in Statistical Physics*, *Physics Reports* **16** 57.

[5] Gardiner C W 1991, *Quantum Noise* (Berlin: Springer).

[6] Plimak L I, Fleischhauer M and Collett M J 1998, unpublished.

[7] Plimak L I, Fleischhauer M and Walls D F 1998, Europhysics Letters **43** 641.

[8] Pauli W and Villars F 1949, *Rev. Mod. Phys.* **21** 434.